International Journal of
INTELLIGENT SYSTEMS AND APPLICATIONS IN ENGINEERING
ISSN:2147-6799 www.ijisae.org Original Research Paper

A New Method for Solving Image Segmentation Problems using Global Optimization

Mariam Ihsan Rmaidh[a]* and Shehab Ahmed Ibrahim[a]

Submitted: 24/01/2023 **Accepted:** 30/03/2023

Abstract

The modified Otsu method with the optimized Filled Function Method is applied in this study to the segmentation of image to establish the appropriate threshold value for segmenting a grayscale image, results were evaluated for some MIR and showed that the partitioning time decreased by almost %70 . and apply the value of Single Peak quality to the Ratio of Noise (PSNR), Error of the Mean Square (MSE), and The Ratio of Noise to Signal (SNR) evaluation criteria for MIR segmentation, results indicate that our method takes little time compared to the conventional OTSU approach, where the real time is used measured in seconds (sec) for the proposed approach and the other algorthms, side by side, without sacrificing hash accuracy.The cons of the huge account are the primary topic of this essay. Due to the old OTSU method's low efficiency, polynomial and Filled Functions method FFM are presented to OTSU. Combining the FFM search optimization algorithm yields the ideal threshold and speeds up computation, which enhances performance segmentation.

Keywords: Image Segmentation, Otsu algorithm, Global Optimization, Filled Function Method.

1. Introduction

Image is segmentation considered the most one of important steps required for processing image research [1; 2]. The fundamental justification is that image segmentation can separate a picture into a number of distinct, homogenous parts that don't overlap in order to improve analysis image [3]. For variety vision of computer applications, including the images that concern medical treat, visionary of robotic, processing of biomedical image, the recognition of patterns, also others, image segmentation is essential. On the basis of the method of base-region, base-edge, base-threshold, and clustering of base-feature, numerous algorithms for image segmentation have been created. Compared to alternative methods, threshold-based segmentation is thought to be preferable due to its simplicity, need for little storage space, accuracy, and speed [4]. During the last few years, many researchers have published a range of different proposed algorithms for image segmentation and optimization. In [5] by putting out a cutting-edge hybrid technique known as the SCABC algorithm, an effort has been made to eliminate the shortcomings of the traditional ABC. The SCABC method combines the algorithm of cosine-sine (SCA) with the colony of bee artificial (ABC) to improve the exploitation and exploitation level in ABC algorithm the traditional. The Foraging Ray of Manta Optimizer (MRFO) algorithm, a heuristic-meta method that models manta rays' foraging activities, has been updated to handle global optimization and multilevel picture segmentation challenges. This algorithm demonstrated its capacity to locate an appropriate solution for various optimization issues. [6]. A version that have been modified of the recently generated the optimizer of equilibrium (EO) is used to segment gray images using multilevel thresholding, and a random path based on the Laplace distribution has been employed for the concentration adjustment of the agents of search around equilibrium filters (best result). This allows the search space to be more diverse. [7]. The local escaping operator (LEO) technique in TSA is integrated with a tunicate swarm algorithm to address the drawbacks of the original TSA (TSA). LEO improves swarm agent convergence and local search effectiveness while preventing search deflation in TSA [8]. To guarantee a better balance between the search of local and global for the algorithm that has been recommended, a new mixture (MPBOA) is suggested in addition to the conventional butterfly optimization technique. BOA's parasitism and mutualism phases were linked with the phase of global , and the phase of parasitism were added to BOA's local phase [9].

[a] *Department of Computer Sciences, University of Kirkuk, College of Computer Sciences and Information Technology, Kirkuk, Iraq*
Email: mullaiq@uokirkuk.edu.iq
**Corresponding Author:*
Department of Computer Sciences, College of Computer Sciences and Information Technology, University of Kirkuk Kirkuk, Iraq
Email: stch21m009@uokirkuk.edu.iq.

In this study, a new method using Global Optimization is used to improve the Otsu method for segmentation by passing a higher-order polynomial $P_n(x)$, between pixels x_i and variance σ^2 to obtain more accurate results in image segmentation.

2. Preliminaries

2.1 Otsu method

In 1979, Japanese researchers proposed the Otsu technique, a global threshold binarization picture system segmentation. The highest interclass between contrast of the image the background and the target were used as the thresholding for this method. Otsu method, often known as the larger variance between categories, is based on a same features. It distinguishes between an images in the foreground and background based on the properties of gray. The difference between the two segments is determined by using the best threshold are bigger[10]. An image is made up of N pixels with grayscale intensities ranging from 1 to 256 in a 2D space. Given that there are fi pixels and gray_level i there was a P ptobability.

$$P(i) = f(i) / N \tag{1}$$

When an image is subjected to bi-level thresholding, pixels are split for two classes: Cf with a threshold for levels of gray [1,..., t] also Cb escorted by a threshold for levels of gray [t+1,..., 256]. Next, the distributions of probability designed to meet the needs of the classes of two at the gray level are

C_f : $P_f/w_f(t), \ldots, P_t/w_f(t)$ and

C_b : $P_{t+1}/w_b(t),\ P_{t+2}/w_b(t), \ldots, P_{256}/w_b(t)$

Where

Weight,Background

$$\mu_b(t) = \frac{\sum_{i=1}^{t} i * P(i)}{w_b(t)} \tag{2}$$

and

Weight,Foreground

$$\mu_f(t) = \frac{\sum_{i=t+1}^{l} i * P(i)}{w_f(t)} \tag{3}$$

also, means of classes $C\,f$ and $C\,b$:

Mean,Background

$$\mu_b(t) = \frac{\sum_{i=1}^{t} i * P(i)}{w_b(t)} \tag{4}$$

and

Mean,Foreground

$$\mu_f(t) = \frac{\sum_{i=t+1}^{l} i * P(i)}{w_f(t)} \tag{5}$$

Let μ_T represent the overall image's mean intensity. It is simple to demonstrate

$$w_f \mu_f = w_b \mu_b \tag{6}$$

$$w_f + w_b = 1 \tag{7}$$

Otsu identified the thresholded image's between-class variation using discriminant analysis as

$$\sigma_B^2 = w_b w_f (\mu_b - \mu_f)^2 \tag{8}$$

Otsu confirmed that for thresholding bi-level, the threshold optimal t* is selected to optimize between-class variance $\sigma_B{}^2$.

$$t^* = \underset{256 > t \geq 1}{\mathrm{Max}} \{ \sigma_B{}^2 (t) \} \tag{9}$$

2.2 Polynomial function

a quadratic, cubic, or quartic function. These are examples of a polynomial's standard form and definition are presented as follows [11; 12].

$$P_n(x) = P_1 x + P_0 + \ldots + P_{n-1} x^{n-1} + P_n x^n \tag{10}$$

where P_1, P_0 ,.., P_n , P_{n-1} are the coefficients of P_n (x) and n, n-1, n-2, ….0 are the powers of x, and all n's are nonnegative integers. Equation (10) was solved just find the coefficients [13].

2.3. Global Optimization

Global optimization problems it can be used for create many different world-real issues in engineering, economics, computer science, and other disciplines. For example:

$$\min_{x \in \Omega} f(x) \tag{10}$$

where $\Omega \in R$ is the domain and f (x) is an objective function [14]. Global optimization issues can be solved using a variety of techniques, including branch and bound methodss [15] and covering algorthms, include space filling curve approaches [16, 17]. Other techniques [18, 19]. These techniques guarantee the solution, but they converge relatively slowly. One of the most crucial approaches in deterministic methods is the auxiliary function approach. In order to switch from the existing local minimizer to a more beneficial one, this approach is created using deterministic search techniques. The auxiliary function can be expressed in a variety of ways, including a method filled function, and method Tunneling [20], Global Descent Method [21; 22; 23].

2.3.1. Filled Function Method

If a function auxiliary $F(x, x_k^*)$ meets criteria below, it was referred to as function filled of the objective function f(x) in minimizer local x_k^*.

• Local maximizer x_k^* of function $F(x, x_k^*)$,

• The function $F(x, x_k^*)$ must not steadfast places at A1 $= \{ x \in \Omega \mid f(x) \geq f(x_k^*), x \neq x_k^* \}$,

• x_k^* if it is not has minimizer global for function f (x), then the function $F(x, x_k^*)$, has steadfast place at A2 = $\{ x \mid f(x) < f(x_k^*) \; x \in \Omega \}$ region.

A first function filled with two parameters was proposed by authores Ge and Qin in 1987 to address the issue (global optimization) in a single minimizer local. Since then, Many significant studies have been done to expand the application of filled functions to other types of issues, including Non-Smooth problem [24;25], optimization problems constrained, systems of Nonlinear Equations [26], and others [27;28]. The following generation of auxiliary function or filled function techniques has recently been created [29;30].

3. Proposed Algorithm

To make a segmentation of medical images that were made with different equipment. This study also shows how to improve the traditional Otsu method of image segmentation by using polynomial equation and Filled Function Method, which shows image segmentation more accurate, specific and fast, which is crucial for the diagnosis of the disease. The stages of the algorithm, as follows:

Algorithm's name (Otsu_FFM)
Input: MRI image
Output: image segmentation
Initial
Step (1): Assume the input is an MRI image.
Step (2): Is to create a gray scale representation of an image.
Step (3): Histogram obtained to MRI image.
Step (4): Obtain the threshold by using Otsu method.
Step (5): Convert threshold from disceret value to curve fitting by using polynomail function .
Step (6): Search the best threshold by using Fillef Function Method.
Step (7): Segmentation image.
End

4. Methodology of research.

In this part, we propose Otsu method with Filled Function Method (Otsu-FFM). This method can be explained into two steps:- 1) separation of the intensity and pixels by using a histogram Figure 1, after finding the pixels, we calculate (σ_B^2) between-class variance by using Equation (8) for each pixel (Otsu method) we represented two vectors pixels (x_i) between-class variance vectors we named it variance (σ^2) as shown in Figure 2.

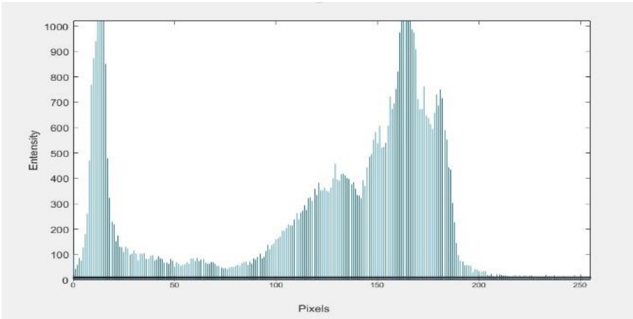

Figure 1 Intensity versus pixels histogram

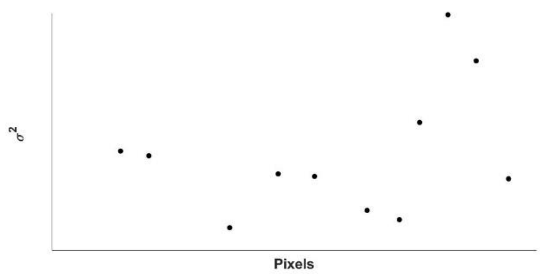

Figure 2: Pixels ($\boldsymbol{x_i}$) and variance value (σ^2)

Based on equation (10), we pass a higher-order polynomial $P_n(x)$ of degree (7) between the pixels (x_i) and variance (σ^2) as shown in Figure 3. (this paper the function objective f(x) was $P_n(x)$ and Ω=[0,255])

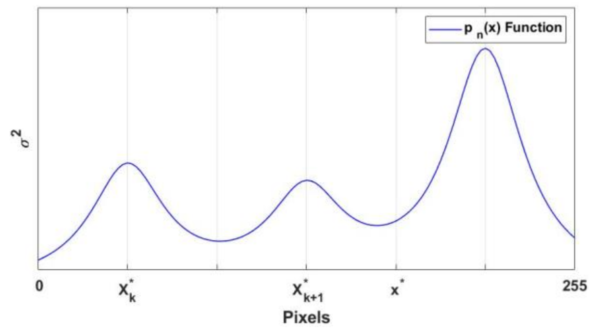

Figure 3: Higher-order polynomial function $\mathbf{P_n(x)}$

Since the method FFM is to find minimizer global, then reverse the function $P_n(x)$ for $-P_n(x)$ which symbolize as $P_n^*(x)$ as it shown in Figure 4.

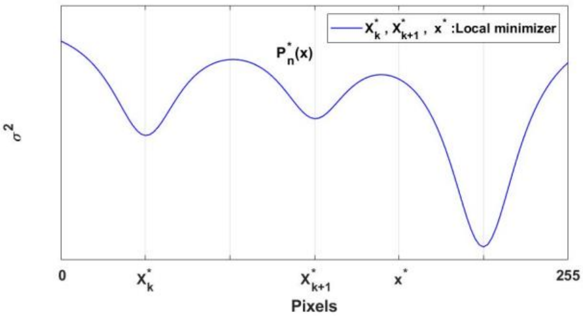

Figure 4: Graph function of the $\mathbf{P_n^*(x)}$

in step 2 the FFM is outlined in the following:-

1- Finding any local minimizer of the objective function $P_n^*(x)$ by make a beginning at any arbitrary pixel in the domain Ω and employing a practical local optimization technique.

2- Creation of the $F(x, x_k^*)$ is established present minimizer x_k^* of $P(x)$, as well as specific point near x_k^* is used to minimize the $F(x, x_k^*)$.

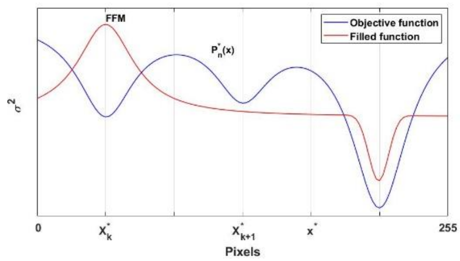

Figure 5: Graph of FFM with $P_n^*(x)$ function.

Finally, a minimizer local of the $F(x, x_k^*)$ is obtained.

3- After finding a minimizer the $F(x, x_k^*)$ which are determined in step 2, then begins with the optimal minimizer of $P_n^*(x)$.

4- The certainly numbers for local minimizers are reduced by repeatedly performing steps 3 and 2 along an image range, we are able to obtain the global minimizer x^* (also known as the optimal threshold) of the $P_n^*(x)$, as illustrated in (Figure 5).

For our methodology, we use FFM, in [24].

$$F(x, x_k^*) = \frac{1}{\alpha + \|x - x_k^*\|^2} h(P_n^*(x) - P_n^*(x_k^*)) \quad (12)$$

$$h(t) = \begin{cases} \sin(\mu t + \frac{\pi}{2}), & t < 0 \\ 1, & t \geq 0 \end{cases}$$

Where t= $P_n^*(x) - P_n^*(x_k^*)$, $\mu > 1$, $\alpha > 0$ are parameters and x_k^* the current local minimizer

We can summerize Otsu_FFM method in this paper in flow chart as shown in Figure 6.

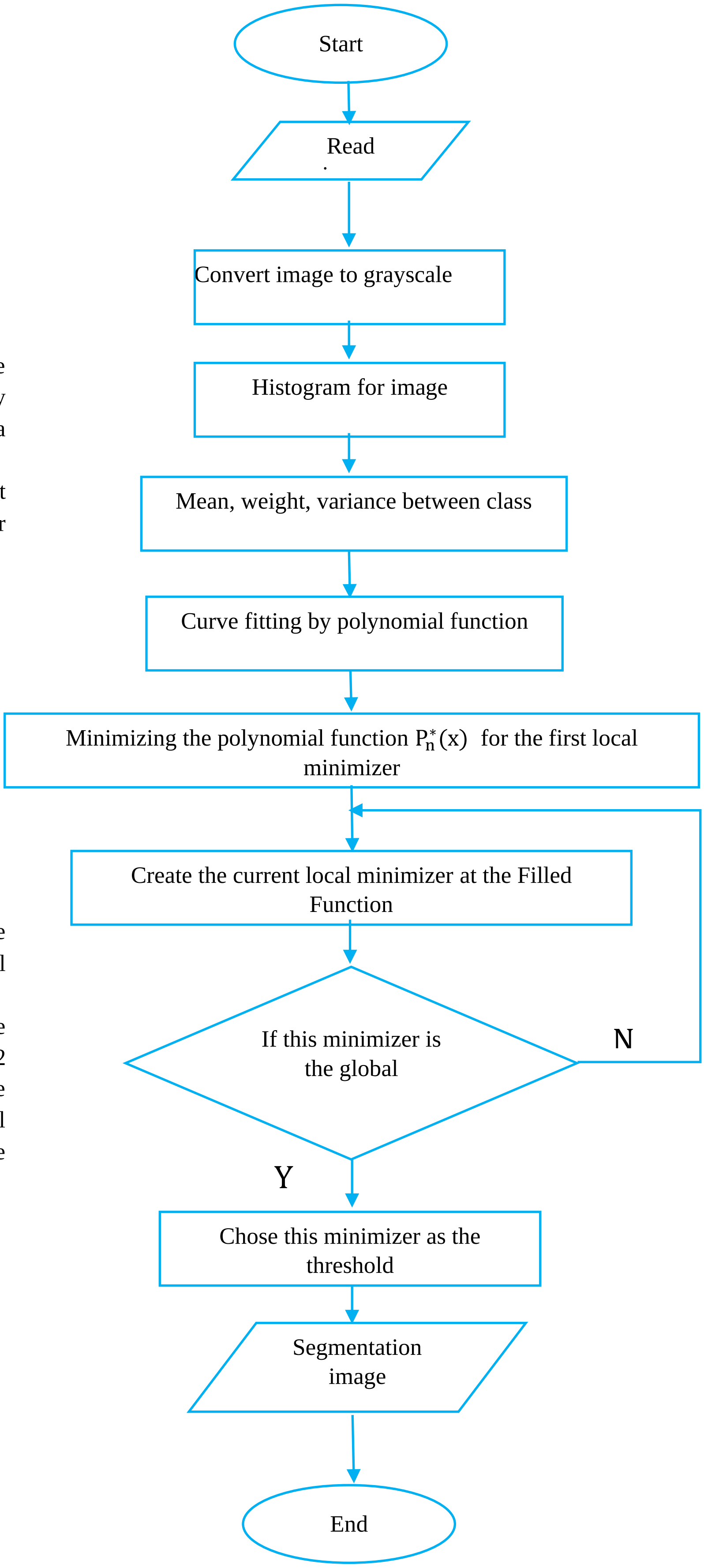

Figure 6: Flowchart of Otsu-FFM method

5. Experimental results

Experimental results are included in this section. The images obtained after each stage are used to calculate the experimental results. The original image can be seen in Figure 7(A). We convert the image to grayscale after obtaining the result of the grayscale image. The segmentation result of the medical image by Otsu's method is shown in Figure 7(B). The result of medical image segmentation by the proposed method, is shown in Figure 7(C). The result of the image is shown in Figure 7(D) by the curved drawing of the proposed method for determining the threshold graphically. The development of the Otsu algorithm is our goal as it finds the threshold in the proposed way more accurately as shown by the curve. As a result, We came up with the idea of converting the threshold value from the discrete value to the (continuous) curve by using the polynomial function that transforms the threshold that was found using the Otsu method to convert it into continuous values. The role of the Filled Function is to find the threshold along the image scale, thus achieving the global optimization of the segmentation based on the threshold.

Image name	Orginal image (A)	Otsu method (B)	Otsu_FFM method (C)	Curve fitting of Otsu_FFM (D)

Image1

Image2

Image3

Image4

Image5

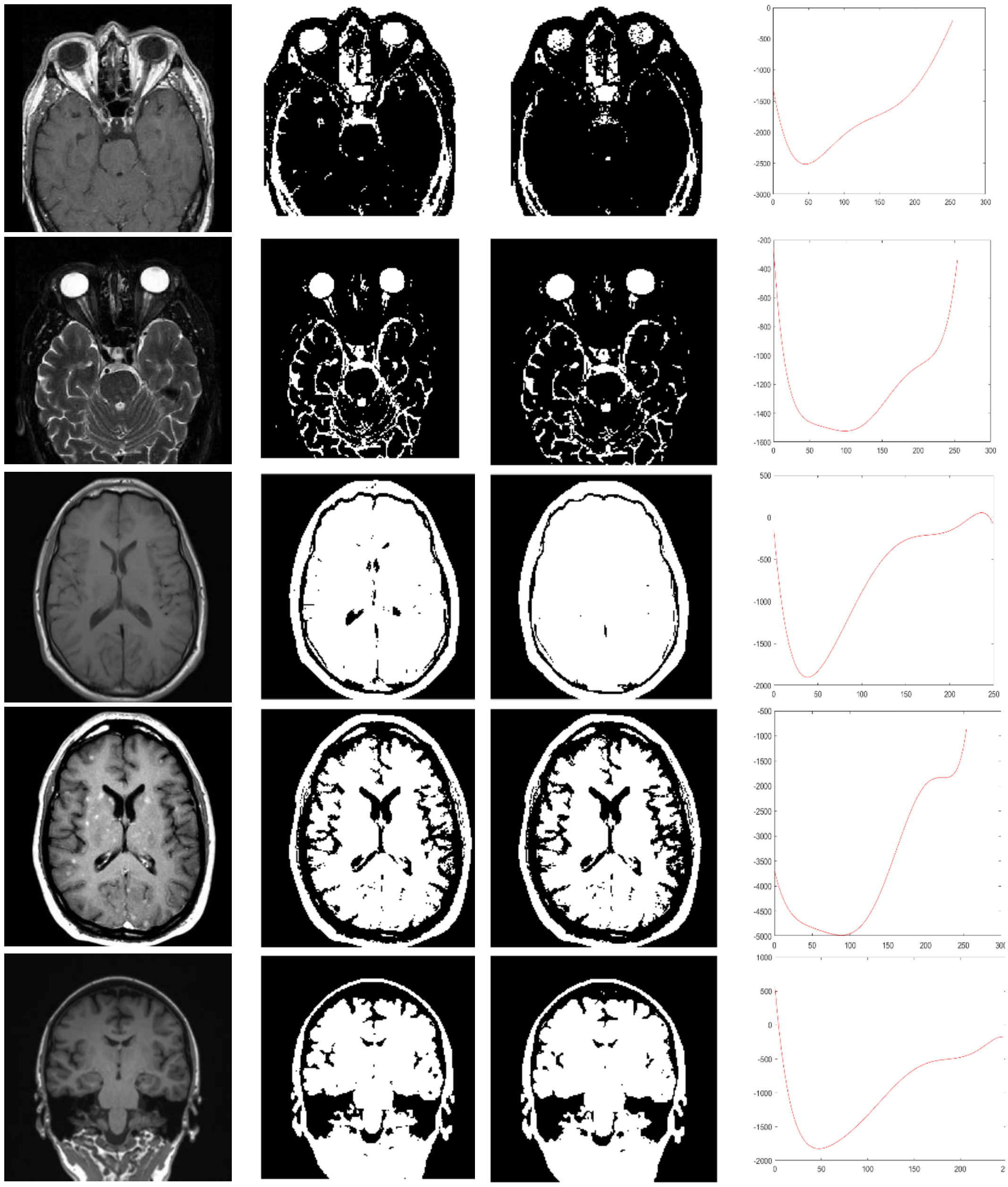

Figure 7: The comparison of Otsu-FFM method and Otsu method

6. Analysis and Performance

SNR, MSE, and PSNR, are the most widely used methods in evaluations. We calculated all of the above-mentioned Figure 7. The following equations are used to compute the outcomes of the above-mentioned values.

$$MSE = \frac{1}{N*M}\sum_{I=0}^{N-1}\sum_{J=0}^{M-1}[|f(i,j) - f(i,j)|.^2] \quad (13)$$

$$SNR = 10log\sum_{I=0}^{N-1}\sum_{J=0}^{M-1}f(i,j).^2 / \sum_{I=0}^{N-1}\sum_{j-1}^{M-1}[f(i,j) - f'(i,j).\hat{}2] \quad (14)$$

$$PSNR = 20\ log\left\{\frac{(255).^2}{MSE}\right\} \quad (15)$$

The result of the (PSNR) and (SNR) tests are provided in decibels (dB).Following the process of segmentation proposed method, the outcomes of the PSNR, SNR, and MSE testing are shown in Table 1.

Table 1: Image quality evaluation (PSNR) ,(SNR) and (MSE) for proposed method Otsu_FFM.

Image name	PSNR (dB)	SNR (dB)	MSE
Image1	5.98779	-2.80976	29.29368
Image2	5.51420	-6.27462	29.14011
Image3	5.94932	-5.04689	29.78154
Image4	5.66198	-1.63652	28.21324
Image5	5.77328	-5.50709	29.65139

Table 2: MSE comparison to the outcomes of other methodologies.

Image name	Otsu_FFM	Otsu	K_means
Image1	29.29368	29.29561	29.33325
Image2	29.14011	29.16074	42.84515
Image3	29.78154	29.82211	45.99591
Image4	28.21324	28.31683	46.71081
Image5	29.65139	29.73304	44.31794

Table 3: Comparison of performance other methodologies in computation time (sec) for the five images selected from the dataset.

Image name	Otsu_FFM	Otsu	K_means	Fuzzy c_means
Image1	0.0224	0.0214	0.3133	1.8657
Image2	0.0215	0.0244	0.3699	2.3361
Image3	0.0334	0.0449	0.5120	7.0356
Image4	0.0298	0.0416	0.6756	7.1701
Image5	0.0448	0.0558	0.4918	6.9090

Table 4: Compared the proposed method threshold with the Otsu method threshold using databset.

Image name	Otsu method threshold	Otsu_FFM method threshold
Image1	53	47
Image2	83	88
Image3	53	38
Image4	89	98
Image5	63	45

7. Conclusions

In this study, we used an MRI scan. We implemented the proposed image segmentation method. These results indicate that the proposed approach has a great ability to segment images more accurately and quickly compared to other methods as shown in Table 4, so we expect that by modifying medical imaging technology, we will be able to significantly reduce the time taken to identify diseases. It is clear from the images resulting from comparison with other methods that they give in the term of accuracy a good, speed,quality and theshold. The proposed method performance of our was measured by determining the average contrast value between the resulting image after segmentation and the image noise ratio (PSNR).We assume 0.7 that the noise calculated as (MSE) becomes less than traditional MSE proposed method Otsu_FFM= 29.29368 and MSE traditional method Otsu =29.29561 and MSE traditional Kmeans = 29.33325, then the results of threshold are compared between the proposed method Ostu_FFM =47 and traditional method Otsu =53 because of curve which obtained from polynomial the threshold of proposed method was more accuracy It also provides an execution speed of 0.0224 seconds for the number one image, which is very low compared to the rest of the methods. Our method can locate tumor sites, but cannot accurately diagnose the disease. Which indicates that this method is better than others in segmentation speed and determinism, and in the future this method requires a machine learning model and an Artificial intelligence (AI) algorithm for disease classification.and also the results indicate that Otsu_FFM Not only can more accurate segmentation results be obtained It is better for suppressing noise by using a filter to reprocess the images before proceeding with the segmentation process, but it also has a lower run time and can Split photos quickly and effectively.

8. Dataset

The dataset comprises of 1,083 MRI pictures of the brain that were acquired from the Harvard Medical School's website. They were gathered in several locations. This includes many illustrations of various varieties of brain tumors.

(URL: http://www.oasis-brains.org/) and the ADNI. data set

(URL: http://med.harvard.edu/AANLIB/), Oasis. data set (URL:https://www.kaggle.com/datasets?search=Brain+MRI&tags=13302-Classification) dataset.

9. Reference

[1] A. K. Rostam, A. M. Murshid, and B. F. Jumaa, "Medical and color images compression using new wavelet transformation," *Int. J. Nonlinear Anal. Appl.*, 2022.

[2] S. A. Ibrahem, S. U. Umar, and A. J. Naji, "Improved image segmentation method based on optimized higher-order polynomial," *Int. J. Nonlinear Anal. Appl*, vol. 14, no. 1, pp. 2701–2715, 2023.

[3] L. Li, L. Sun, Y. Xue, S. Li, X. Huang, and R. F. Mansour, "Fuzzy multilevel image thresholding based on improved coyote optimization algorithm," *IEEE Access*, vol. 9, pp. 33595–33607, 2021.

[4] M. Abdel-Basset, V. Chang, and R. Mohamed, "A novel equilibrium optimization algorithm for multi-thresholding image segmentation problems," *Neural Comput. Appl.*, vol. 33, no. 17, pp. 10685–10718, 2021.

[5] S. Gupta and K. Deep, "Hybrid sine cosine artificial bee colony algorithm for global optimization and image segmentation," *Neural Comput. Appl.*, vol. 32, no. 13, pp. 9521–9543, 2020.

[6] E. H. Houssein, B. E. Helmy, D. Oliva, A. A. Elngar, and H. Shaban, "A novel black widow optimization algorithm for multilevel thresholding image segmentation," *Expert Syst. Appl.*, vol. 167, p. 114159, 2021.

[7] S. K. Dinkar, K. Deep, S. Mirjalili, and S. Thapliyal, "Opposition-based Laplacian equilibrium optimizer with application in image segmentation using multilevel thresholding," *Expert Syst. Appl.*, vol. 174, p. 114766, 2021.

[8] E. H. Houssein, B. E.-D. Helmy, A. A. Elngar, D. S. Abdelminaam, and H. Shaban, "An improved tunicate swarm algorithm for global optimization and image segmentation," *IEEE Access*, vol. 9, pp. 56066–56092, 2021.

[9] S. Sharma, A. K. Saha, A. Majumder, and S. Nama, "MPBOA-A novel hybrid butterfly optimization algorithm with symbiosis organisms search for global optimization and image segmentation," *Multimed. Tools Appl.*, vol. 80, no. 8, pp. 12035–12076, 2021.

[10] C. Huang, X. Li, and Y. Wen, "AN OTSU image segmentation based on fruitfly optimization algorithm," *Alexandria Eng. J.*, vol. 60, no. 1, pp. 183–188, 2021.

[11] S. C. Gupta and V. K. Kapoor, *Fundamentals of mathematical statistics*. Sultan Chand & Sons, 2020.

[12] M. Nagahara, *Sparsity methods for systems and control*. now Publishers, 2020.

[13] Y. Zhang, D. Chen, and C. Ye, *Deep neural networks: wasd neuronet models, algorithms, and applications*. CRC Press, 2019.

[14] I. A. Masoud Abdulhamid, A. Sahiner, and J. Rahebi, "New auxiliary function with properties in nonsmooth global optimization for melanoma skin cancer segmentation," *Biomed Res. Int.*, vol. 2020, 2020.

[15] L. Abualigah, A. Diabat, P. Sumari, and A. H. Gandomi, "A novel evolutionary arithmetic optimization algorithm for multilevel thresholding segmentation of covid-19 ct images," *Processes*, vol. 9, no. 7, Jul. 2021, doi: 10.3390/pr9071155.

[16] L. Abualigah, A. Diabat, P. Sumari, and A. H. Gandomi, "A novel evolutionary arithmetic optimization algorithm for multilevel thresholding segmentation of covid-19 ct images," *Processes*, vol. 9, no. 7, p. 1155, 2021.

[17] J. Tang, G. Liu, and Q. Pan, "A review on representative swarm intelligence algorithms for solving optimization problems: Applications and trends," *IEEE/CAA J. Autom. Sin.*, vol. 8, no. 10, pp. 1627–1643, 2021.

[18] D. Yousri, M. Abd Elaziz, and S. Mirjalili, "Fractional-order calculus-based flower pollination algorithm with local search for global optimization and image segmentation," *Knowledge-Based Syst.*, vol. 197, p. 105889, 2020.

[19] N. Safaei, O. Smadi, A. Masoud, and B. Safaei, "An automatic image processing algorithm based on crack pixel density for pavement crack detection and classification," *Int. J. Pavement Res. Technol.*, vol. 15, no. 1, pp. 159–172, 2022.

[20] M. Poojary and Y. Srinivas, "Optimization Technique Based Approach for Image Segmentation.," *Curr. Med. Imaging*, 2022.

[21] T. Fang, J. Yuan, R. Yin, and C. Wu, "A Novel Image Edge Detection Method Based on the Asymmetric STDP Mechanism of the Visual Path," *Wirel. Commun. Mob. Comput.*, vol. 2022, 2022.

[22] R. Mohakud and R. Dash, "Skin cancer image segmentation utilizing a novel EN-GWO based hyper-parameter optimized FCEDN," *J. King Saud Univ. Inf. Sci.*, 2022.

[23] M. Abdel-Basset, R. Mohamed, and M. Abouhawwash, "A new fusion of whale optimizer algorithm with Kapur's entropy for multi-threshold image segmentation: analysis and validations," *Artif. Intell. Rev.*, pp. 1–71, 2022.

[24] Y. Zhang, L. Zhang, and Y. Xu, "New filled functions for nonsmooth global optimization," *Appl. Math. Model.*, vol. 33, no. 7, pp. 3114–3129, 2009.

[25] A. Sahiner, H. Gokkaya, and T. Yigit, "A new filled function for nonsmooth global optimization," in *AIP conference proceedings*, 2012, vol. 1479, no. 1, pp. 972–974.

[26] L. Yuan, Z. Wan, Q. Tang, and Y. Zheng, "A class of parameter-free filled functions for box-constrained system of nonlinear equations," *Acta Math. Appl. Sin. English Ser.*, vol. 32, no. 2, pp. 355–364, 2016.

[27] F. Wei, Y. Wang, and H. Lin, "A new filled function method with two parameters for global optimization," *J. Optim. Theory Appl.*, vol. 163, pp. 510–527, 2014.

[28] H. Lin, Y. Gao, and Y. Wang, "A continuously

differentiable filled function method for global optimization," *Numer. Algorithms*, vol. 66, pp. 511–523, 2014.

[29] N. Yilmaz and A. Sahiner, "New global optimization method for non-smooth unconstrained continuous optimization," in *AIP Conference Proceedings*, 2017, vol. 1863, no. 1, p. 250002.

[30] A. Sahiner and S. A. Ibrahem, "A new global optimization technique by auxiliary function method in a directional search," *Optim. Lett.*, vol. 13, pp. 309–323, 2019.